Evidence for Crystalline Water and Ammonia Ices on Pluto's Satellite Charon

Michael E. Brown[1] and Wendy M. Calvin[2]

Observations have resolved the satellite Charon from its parent planet Pluto, giving separate spectra of the two objects from 1.0 to 2.5 micrometers. The spectrum of Charon is found to be different from that of Pluto, with water ice in crystalline form covering most of the surface of the satellite. In addition, an absorption feature in Charon's spectrum suggests the presence of ammonia ices. Ammonia ice–water ice mixtures have been proposed as the cause of flowlike features observed on the surfaces of many icy satellites. The existence of such ices on Charon may indicate geological activity in the satellite's past.

Pluto's satellite Charon orbits Pluto so closely that, even though it is only five times fainter than Pluto, Charon's existence was not discovered until 1978 (*1*). Even after discovery, the small separation between the two objects has made separate study of them difficult. Most of our current knowledge about the composition of Charon comes from observations of a series of mutual Pluto-Charon eclipses between 1985 and 1990. In two such series of eclipses, Pluto and Charon were observed together, and then Pluto was observed separately as it completely occulted Charon. Subtraction of the two observations then yielded the brightness of Charon. By performing these observations at a small number of wavelengths over the near-infrared region, a low-resolution spectrum of Charon was synthesized. These spectra showed evidence for a surface covered in water ice, much like the satellites of the giant planets and unlike the surface of Pluto (*2*). The possible existence of materials other than water ice was also considered, but the crudeness of the data did not permit any resolution of the issue (*3*).

Observing Pluto and Charon separately from the ground is difficult. The maximum separation between the two objects is currently 0.9 arc seconds, and typical atmosphere-induced blurring at the Keck telescope on Mauna Kea is ~0.5 arc seconds in the infrared. On an exceptional night of 0.3–arc second atmospheric seeing, the two objects were distinct, and we obtained well-separated near-infrared images (Fig. 1) (*4*) and spectra of the two objects (Figs. 2 and 3) (*5*). The lack of any common spectral features between Pluto and Charon demonstrates that the final spectrum of Charon is separated from Pluto.

The spectrum of Pluto has previously been studied in detail (*6*). The spectrum of Charon has been known previously to be dominated by the signature of water ice (*2*), but the crudeness of the previous spectrum prevented further analysis. As expected, our spectrum of Charon is also dominated by the 1.5- and 2.0-μm absorption bands of water ice. The additional appearance of the small 1.65-μm absorption feature redward of the main 1.5-μm absorption demonstrates that the surface water ice is unexpectedly crystalline, rather than amorphous, in form (*7*). At the ~50 K temperature of Charon, crystalline water ice is turned into amorphous form under bombardment from solar ultraviolet radiation (*8*). The presence of crystalline ice on the surface of Charon suggests that continuous micrometeorite impact vaporization and the subsequent recondensation of crystalline ice on the surface of Charon proceed faster than the radiation-induced transformation to amorphous ice. The presence of crystalline water ice on all of the well-studied icy satellites in the outer solar system (*9*) confirms that a ubiquitous mechanism such as impacts must be responsible.

A model consisting of only crystalline water ice and a dark, spectrally neutral material (*10*) reproduces all of the major features of our spectrum of Charon except at the 2.2-μm peak and longward of 2.3 μm. Although the inclusion of larger grain sizes of water ice could contribute to a better fit beyond 2.3 μm, the suppression of the 2.2-μm peak in Charon cannot be attributed to water ice and requires additional absorbing materials on the surface. To identify the 2.2-μm absorption, we considered all of the ices previously observed on or proposed for solar system bodies and the interstellar medium. In addition, we considered all other simple combinations of H, C, N, and O, the four most abundant molecule-forming elements in the solar system, and more complex hydrocarbons such as tholins and kerogens, which have long been considered plausible causes for the low-albedo surfaces in the outer solar system. Given the recent reports of hydrated minerals on the icy satellites of Jupiter (*11*), we also considered all common terrestrial rock-forming minerals. Of all of these possible constituents, only HCN, NH_3, $NH_3 \cdot 2H_2O$ (ammonia hydrate), and alumino silicate clays have absorption features in the 2.2-μm region (Fig. 4). We constructed spectral models using combinations of these compounds, water ice, and a dark neutral material (*12*) and compared them with the spectrum of Charon. These comparisons show that HCN cannot reproduce the abrupt flattening of the 2.2-μm peak that is observed on Charon and that the clays have band centers displaced to shorter wavelengths than observed on Charon. Ammonia and ammonia hydrate individually have absorption features too narrow to reproduce the Charon spectrum, but a combination of the two produces an absorption that matches both the depth and location of the observed Charon absorption. In addition, all other absorption features of ammonia and ammonia hydrate correspond to strong water ice absorptions, so the spectral signature of water ice is not disturbed elsewhere, as seen in a model consisting of water ice (44% surface coverage), ammonia (1%), ammonia hydrate (24%), and a dark neutral material (32%) (Fig. 3). Like crystalline water ice, ammonia hydrate ices are destroyed by radiation (*13*). Whatever process allows the crystalline ices to exist on the surface of Charon could also be responsible for the continued appearance of ammonia even in the presence of radiation. The remaining discrepancies between the model and the data and the use of a combination of pure ammonia and ammonia hydrate suggest that Charon may have a different hydrate structure (some inclusion of $NH_3 \cdot H_2O$). Unfortunately, a systematic spec-

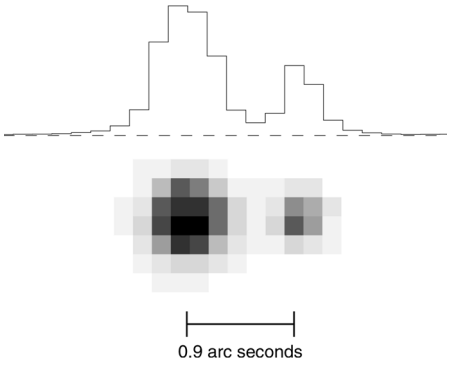

Fig. 1. Images of Pluto (**left**) and its satellite Charon (**right**) at the K band (~2 μm). The objects are spaced by 0.90 arc seconds and are separated in the 0.30–arc second seeing. The histogram above the image gives a trace of the intensity through the center of the system, showing how little of the light from Pluto contaminates the spectrum of Charon.

[1]Division of Geological and Planetary Sciences, California Institute of Technology, Pasadena, CA 91125, USA. [2]Department of Geological Sciences, University of Nevada–Reno, Reno, NV 89557, USA.

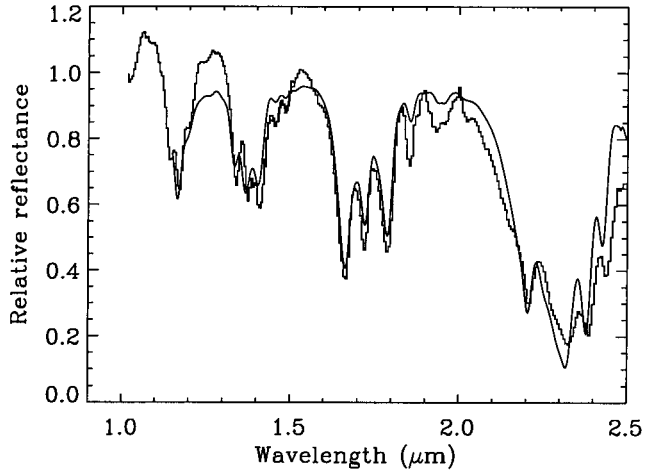

Fig. 2 (left). The near-infrared spectrum of Pluto. The histogrammed points give the data, scaled to a value of unity at a wavelength of 1.5 μm, and the smooth line is a reflectance spectrum of pure methane ice from Fink and Sill (*7*). The surface of Pluto is also known to contain N_2 and CO, but the weak spectral features due to these ices are not readily visible at this spectral resolution.

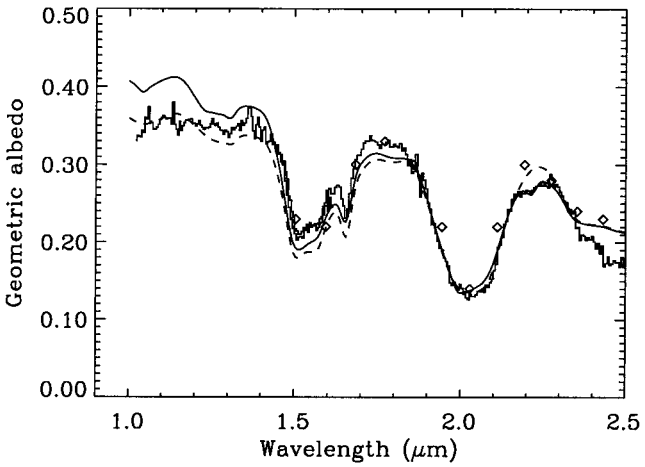

Fig. 3 (right). The near-infrared geometric albedo spectrum of Charon. The histogram gives the data, which has been scaled to the geometric albedo of Charon derived by Roush (*3*). The dashed line shows a model consisting of only water ice and a dark neutral absorber. The solid line is a model in which ammonia and ammonia hydrate ices have been added to the water ice and neutral absorber.

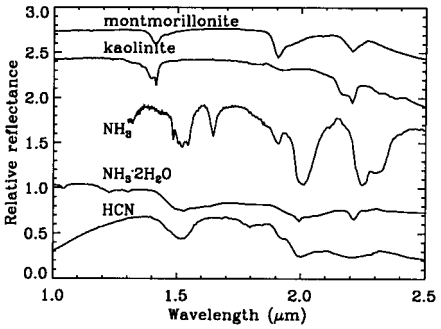

Fig. 4. Spectra of candidates for the 2.2-μm absorption seen on Charon (*20*). Montmorillonite and kaolinite are alumino silicate clays.

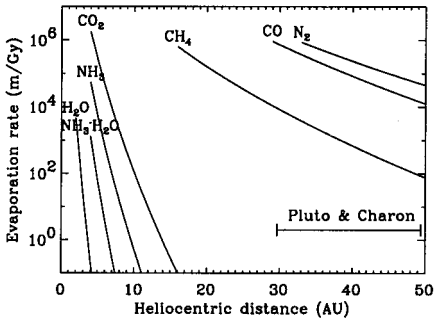

Fig. 5. Evaporation rates (in meters per billion years) of ices from the surface of an object in the outer solar system. The rates were calculated by assuming equilibrium between the temperature-dependent vapor pressure of the ice and the pressure of the escaping gas immediately above the surface of the object (*21*). AU, astronomical units.

troscopic study of ammonia hydrates has not been performed at these wavelengths. It is known, however, that hydration of ammonia will shift the 2.2-μm absorption feature to a shorter wavelength and broaden the feature (*14*). The model fit also has discrepancies at the bottom of the 2.0-μm trough and a higher albedo in the region longward of 2.3 μm, where additional absorbers may be needed. In addition, the model continuum level shortward of 1.5 μm is too high, suggesting that the dark surface component is optically red, as has been inferred for many low-albedo asteroids and other dark surfaces in the solar system (*15*).

The existence of nitrogen in the form of ammonia ices on the surface of Charon is a marked contrast to the surface of Pluto, where the nitrogen exists in molecular form. This difference may be due to the high volatility of molecular nitrogen and the relative sizes of these outer solar system bodies. In the absence of gravity, bodies at the ~50 K temperature of Pluto and Charon would sublime about 1000 km of molecular nitrogen over the age of the solar system (Fig. 5). Pluto, with a radius of 1195 km, a mass of 1.5×10^{22} kg, and therefore an escape velocity of 1.3 km s^{-1}, is massive enough to retain the nitrogen as an atmosphere and a frost surface. Charon, however, owing to its smaller size—a radius of 593 km and a mass of 3.3×10^{21} kg—and hence smaller escape velocity of 0.86 km s^{-1}, is ~2 million times less efficient at retaining an atmosphere against Jean's escape (*16*) so the volatile ices seen on Pluto (including CO and CH_4) will be sublimed from Charon over time scales as short as millions of years. If this hypothesis for the origin of the difference in surface composition of Pluto and Charon is correct, a prediction would be that underneath a layer of condensed volatile frosts, the surface of Pluto is much like that of Charon.

Ammonia ices have been predicted to be an important component of icy satellites in the outer solar system (*17*). The discovery by Voyager that even relatively small satellites, with interiors too cold to melt pure ice, have had complex geologic histories led to the realization that ammonia-water mixtures, because of their lower melting temperatures and higher viscosities than pure water, may be responsible for the activity seen on these bodies (*18*). Charon is about the size of the uranian satellites Ariel (579 km) and Umbriel (586 km), both of which exhibit a variety of surface geologic units including cratered plains and fault valleys whose floors suggest infilling by erupted and flowing materials similar to terrestrial volcanic flows (*19*). Charon should have experienced similar amounts of accretional heating in the past, in addition to any extra heating from tidal evolution of the Pluto-Charon system, so similar geological activity on this body is expected. The detection of ammonia ices on Charon suggests that such ices may play an important role in geological activity on icy bodies in the outer solar system.

References and Notes

1. J. W. Christy, *IAU Circ.* **3241**, 1 (1978).
2. R. L. Marcialis, G. H. Rieke, L. A. Lebofsky, *Science* **237**, 1349 (1987); M. W. Buie, D. P. Cruikshank, L. A. Lebofsky, E. F. Tedesco, *Nature* **329**, 522 (1987).
3. T. L. Roush, *Icarus* **108**, 243 (1994).
4. Images and spectra of Pluto and Charon were obtained at the Keck telescope with NIRC, the facility's near-infrared imaging spectrograph. Images were acquired on 28 May 1999 at 10:20 UT. For imaging, a K band filter (covering ~2 to 2.4 μm) was used; it took two 10-s images with Pluto dithered by 10 arc seconds between the images. Figure 1 shows the difference of the two images. The NIRC pixels are 0.15 arc seconds, and the separation of Pluto and Charon at the time of the observations was 0.899 arc seconds, or about 6 pixels. The full width at half maximum of the atmospheric turbulence–induced

blurring, measured from a nearby star immediately before the start of the Pluto observations, was 0.30 arc seconds.

5. Spectra of Pluto and Charon were obtained on 28 May 1999 from 10:35 until 11:37 UT. The objects were acquired in direct imaging mode, and then, with the telescope tracking at the predicted Pluto rate on the sky, the image rotator was positioned so that Pluto and Charon fell into the 0.37–arc second–wide slit. Data acquisition and analysis were performed in a manner described in detail by M. E. Brown (*Astron. J.*, in press). Two spectral settings were required to cover the full spectral range. We acquired a total of 300 s of exposure in the HK band (1.5 to 2.5 μm) and 100 s of exposure in the JH band (1.0 to 1.6 μm). Even in the exceptionally good seeing present at the time of the observations, some light from Pluto is contained in the raw spectrum of Charon (Fig. 1). To eliminate this contribution, we subtracted the spectrum of Pluto from an equidistant point on the non-Charon side from the spectrum of Charon. This correction was equal to ~10% of the measured light from Charon. To provide a correction for atmospheric extinction, we measured the spectrum of the nearby F8V star SAO 181258 and ratioed the flux to that expected from a blackbody of equivalent temperature. This calibration star should have spectral features almost identical to those from the sun at these wavelengths [A. Lancon and B. Rocca-Volmerange, *Astron. Astrophys. Suppl. Ser.* **96**, 593 (1992)]; any spurious spectral features caused by the use of this calibrator will be smaller than a few percent of the total signal and will not be visible in the data. The spectra were scaled to absolute albedo from the data of T. L. Roush, D. P. Cruikshank, J. B. Pollack, E. F. Young, and M. J. Bartholomew [*Icarus* **119**, 214 (1996)].
6. See review by D. P. Cruikshank *et al.*, in *Pluto and Charon*, S. A. Stern and D. J. Tholen, Eds. (Univ. of Arizona Press, Tucson, AZ, 1997), pp. 221–267.
7. U. Fink and G. T. Sill, in *Comets*, L. Wilkening, Ed. (Univ. of Arizona Press, Tucson, AZ, 1982), pp. 172–202.
8. Simple extrapolation from the laboratory results [A. Kouchi and T. Kuroda, *Nature* **344**, 134 (1990)] suggests that the time scale for amorphization at Charon's distance from the sun could be as short as 1 hour; however, the weak ultraviolet flux of the sun compared with the laboratory lamp used could make the time scale orders of magnitude longer.
9. W. M. Grundy, M. W. Buie, J. A. Stansberry, J. R. Spencer, B. Schmitt, *Icarus*, in press.
10. We modeled the geometric albedo of an object consisting of spatially distinct regions of pure water ice and a dark neutral material using the absorption coefficients of crystalline water at a temperature of 50 K as measured by W. M. Grundy and B. Schmitt [*J. Geophys Res.* **103**, 25809 (1998)] and the reflectance spectroscopic theory of B. Hapke [*J. Geophys. Res.* **86**, 3039 (1981)]. We assumed grain sizes of 20 μm, which gave the best fit to the depths of the different ice bands.
11. T. B. McCord *et al.*, *J. Geophys. Res.* **104**, 11827 (1999); F. P. Fanale *et al.*, *Icarus* **139**, 179 (1999).
12. The geometric albedo models were constructed by using spatially segregated mixtures combining crystalline water ice, a dark neutral material, and one of the compounds with a 2.2-μm absorption (HCN, NH_3, $NH_3{\cdot}2H_2O$, or alumino silicate clays). A grid search was performed checking all possible ratios of surface coverage of the various components and grain sizes from 2 μm up to 1 mm. Larger grain sizes were not considered because they cause band depths to be too large. For some of the ices, optical constants are not available, so we resorted to scaling the pure reflectance spectra instead of calculating the geometric albedo. Our preferred model uses 20-μm water ice grains at a temperature of 50 K mixed with a dark neutral absorber with an albedo of 4% and ammonia and ammonia hydrate.
13. L. J. Lanzerotti, W. L. Brown, K. J. Marcantonio, R. E. Johnson, *Nature* **312**, 139 (1984).
14. B. Schmitt, E. Quirico, F. Trotta, W. M. Grundy, in *Solar System Ices*, B. Schmitt, C. de Bergh, M. Festou, Eds. (Kluwer Academic, Boston, MA, 1998), pp. 199–241.
15. B. N. Khare *et al.*, *Icarus* **79**, 350 (1989); B. N. Khare *et al.*, *Icarus* **103**, 290 (1993).
16. J. W. Chamberlain and D. M. Hunten, *Theory of Planetary Atmospheres* (Academic Press, Orlando, FL, 1987).
17. J. S. Lewis, *Icarus* **15**, 174 (1971).
18. D. J. Stevenson, *Nature* **298**, 142 (1982); P. M. Schenk, *J. Geophys. Res.* **96**, 1887 (1991); J. S. Kargel, S. K. Croft, J. I. Lunine, J. S. Lewis, *Icarus* **89**, 93 (1992); W. B. Durham, S. H. Kirby, L. A. Stern, *J. Geophys. Res.* **98**, 17667 (1993).
19. S. K. Croft and L. A. Soderblom, in *Uranus*, J. T. Bergstralh, E. D. Miner, M. S. Matthews, Eds. (Univ. of Arizona Press, Tucson, AZ, 1997), pp. 561–628.
20. The spectra of montmorillonite and kaolinite are courtesy of Roger Clark, that of NH_3 is from (*7*), that of $NH_3{\cdot}2H_2O$ is from R. H. Brown, D. P. Cruikshank, A. T. Tokumaga, R. G. Smith, and R. N. Clark [*Icarus* **74**, 262 (1988)], and that of HCN is from D. P. Cruikshank *et al.* [*Icarus* **94**, 345 (1991)].
21. The time rate of sublimation is calculated by assuming equilibrium between the temperature-dependent vapor pressure of the ice [D. R. Lide, Ed., *CRC Handbook of Chemistry and Physics* (CRC Press, Boca Raton, FL, ed. 77, 1996)] and the pressure of the escaping gas immediately above the surface of the object. The temperature is calculated by assuming radiative equilibrium between a pure blackbody and the incoming sunlight.
22. We thank R. Clark and D. Cruikshank for making their spectral data available to us and E. Young and D. Cruikshank for insightful comments on the manuscript. M.E.B. is an Alfred P. Sloan Research Fellow. These data were obtained at the W. M. Keck Observatory, which is operated as a scientific partnership among the California Institute of Technology, the Universities of California, and NASA. The observatory was made possible by the financial support of the W. M. Keck Foundation.

23 September 1999; accepted 6 December 1999

Evidence for a Low-Density Universe from the Relative Velocities of Galaxies

R. Juszkiewicz,[1]* P. G. Ferreira,[1,2,3]† H. A. Feldman,[4] A. H. Jaffe,[5] M. Davis[5]

The motions of galaxies can be used to constrain the cosmological density parameter Ω and the clustering amplitude of matter on large scales. The mean relative velocity of galaxy pairs, estimated from the Mark III survey, indicates that $\Omega = 0.35^{+0.35}_{-0.25}$. If the clustering of galaxies is unbiased on large scales, $\Omega = 0.35 \pm 0.15$, so that an unbiased Einstein–de Sitter model ($\Omega = 1$) is inconsistent with the data.

The mean relative velocity for a pair of galaxies at positions $\vec{r}_1$ and $\vec{r}_2$ is $\vec{u}_{12} = H\vec{r}$, where $\vec{r} = \vec{r}_1 - \vec{r}_2$ and the constant of proportionality $H = 100h$ km s^{-1} Mpc^{-1} is the Hubble parameter (*1, 2*). The quantity $0.6 < h < 1$ parameterizes uncertainties in H measurements. This law is an idealization, followed by real galaxies only on sufficiently large scales, corresponding to a uniform mass distribution. On smaller scales, the gravitational field induced by galaxy clusters and voids generates local deviations from the Hubble flow, called peculiar velocities. Correcting for this effect gives $\vec{u}_{12} = H\vec{r} + v_{12}\vec{r}/r$. The quantity $v_{12}(r)$ is called the mean pairwise streaming velocity. In the limit of large r, $v_{12} = 0$. In the opposite limit of small separations, $u_{12}(r) = 0$ (virial equilibrium). Hence, at intermediate separations, $v_{12} < 0$ and we can expect to observe gravitational infall, or the "mean tendency of well-separated galaxies to approach each other" (*3*). In a recent paper, we derived an expression, relating v_{12} to cosmological parameters (*4*); in another, using Monte Carlo simulations, we showed how v_{12} can be measured from velocity-distance surveys of galaxies (*5*). Our purpose here is to estimate $v_{12}(r)$ from observations and constrain the cosmological density parameter Ω.

The statistic we consider was introduced in the context of the Bogoliubov-Born-Green-Kirkwood-Yvon (BBGKY) kinetic theory describing the dynamical evolution of a self-gravitating collection of particles (*3, 6*). One of the BBGKY equations is the pair conservation equation, relating the time evolution of v_{12} to $\xi(r)$, the two-point correlation function of spatial fluctuations in the fractional matter density contrast (*3*). Its solution is well approximated by (*4*)

$$v_{12}(r) = -\frac{2}{3} Hr\Omega^{0.6}\bar{\bar{\xi}}(r)[1 + \alpha\bar{\bar{\xi}}(r)] \quad (1)$$

$$\bar{\bar{\xi}}(r) = \frac{3\int_0^r \xi(x)x^2dx}{r^3[1 + \xi(r)]} \quad (2)$$

where $\alpha = 1.2 - 0.65\gamma$, $\gamma = -(d \ln \xi/d \ln$

[1]Département de Physique Théorique, Université de Genève, CH-1211 Genève, Switzerland. [2]Theory Group, CERN, CH-1211 Genève 23, Switzerland. [3]CENTRA, Instituto Superior Tecnico, Lisboa 1096 Codex, Portugal. [4]Department of Physics and Astronomy, University of Kansas, Lawrence, KS 66045, USA. [5]Center for Particle Astrophysics, University of California, Berkeley, CA 94720, USA.

*On leave from Copernicus Astronomical Center, 00-716 Warsaw, Poland.

†To whom correspondence should be addressed. E-mail: pgf@astro.ox.ac.uk